Arabian Journal of Chemistry (2019) **12**, 1148–1158

King Saud University

Arabian Journal of Chemistry

www.ksu.edu.sa
www.sciencedirect.com

ORIGINAL ARTICLE

Magnetically modified nanogold-biosilica composite as an effective catalyst for CO oxidation

Veronika Holišová [a,*], Marta Natšinová [a], Gabriela Kratošová [a], Žaneta Chromčáková [b], Adam Schröfel [c,d], Ivo Vávra [e], Ondřej Životský [f], Ivo Šafařík [g,h], Lucie Obalová [b]

[a] *Nanotechnology Centre, VŠB – Technical University of Ostrava, 17. listopadu 15/2172, 708 33 Ostrava – Poruba, Czech Republic*
[b] *Institute of Environmental Technology, VŠB – Technical University of Ostrava, 17. listopadu 15/2172, 708 33 Ostrava – Poruba, Czech Republic*
[c] *Faculty of Science, Institute of Cellular Biology and Pathology, Charles University, Albertov 6, Prague 2, Czech Republic*
[d] *Max Planck Institute of Molecular Cell Biology and Genetics, Pfotenhauer straße 108, 01307 Dresden, Germany*
[e] *Institute of Electrical Engineering, Slovak Academy of Sciences, Bratislava, Slovak Republic*
[f] *Department of Physics, Faculty of Electrical Engineering and Computer Science, VŠB – Technical University of Ostrava, 17. listopadu 15/2172, 708 33 Ostrava-Poruba, Czech Republic*
[g] *Department of Nanobiotechnology, Biology Centre, ISB, Academy of Sciences of the Czech Republic, Na Sadkach 7, 370 05 Ceske Budejovice, Czech Republic*
[h] *Regional Centre of Advanced Technologies and Materials, Palacky University, Slechtitelu 27, 783 71 Olomouc, Czech Republic*

Received 26 September 2018; accepted 2 December 2018
Available online 10 December 2018

KEYWORDS

Biosynthesis;
Nanogold-biosilica;
Ferrofluid;
Catalysis;
Carbon monoxide

Abstract The temperature-dependent biosynthesis of gold nanoparticles (AuNP) using diatom cells of *Diadesmis gallica* was successfully performed. The resulting biosynthesis product was a bionanocomposite containing AuNP (app. 20 nm) subsequently anchored on the silica surface of diatomaceous frustules. As-prepared nanogold-biosilica composite was tested as catalyst in the oxidation of carbon monoxide using gas chromatograph with thermal conductivity detector. For catalytic activity enhancement, bionanocomposite was magnetically modified by ferrofluid using two different methods, i.e., with and without the use of methanol. The oxidation of CO at 300 °C was 58–60% in the presence of nanogold-biosilica composites. CO conversion at 300 °C was only 15% over magnetically responsive sample modified in the presence of methanol. On the other hand, complete CO conversion was reached over direct (without methanol) magnetically modified nanogold-biosilica composite at 330 °C (GHSV = 60 l g^{-1} h^{-1}). Our results show, that the type of magnetic modification can influence the catalytic activity of bionanocomposite. The best catalytic

* Corresponding author.
E-mail address: HolisovaVeronika@seznam.cz (V. Holišová).
Peer review under responsibility of King Saud University.

Production and hosting by Elsevier

https://doi.org/10.1016/j.arabjc.2018.12.002

effect in CO conversion established direct magnetically modified nanogold-biosilica composite.

1. Introduction

Carbon monoxide (CO) is a tasteless, odourless, non-irritating but toxic gas which affects the oxygen transport in the tissue by creating of carboxyhemoglobin (COHb). Therefore, CO has negative impacts on the cellular respiration in the human body. This toxic gas is produced by incomplete combustion of substances containing carbon. Motor vehicles, combustion appliances, e.g. heating units, in which partial combustion of oils, coal, wood, kerosene and other fuels generate CO are the main sources (Prockop and Chichkova, 2007). Currently, poor heat resistance of a catalyst in motor vehicles (catalyst destruction due to high temperatures) leads to a constant pressure to develop new effective catalysts for CO oxidation at lower temperatures around 100 °C, especially prior to the release of toxic CO into the atmosphere.

Gold was considered as catalytically inactive for a long time until the pioneering work of Haruta changed the view on the use of gold in catalysis (Haruta et al., 1987). He showed that well-dispersed nanosized gold particles supported on metal oxides catalyse CO oxidation at temperatures as low as −77 °C. Since this Haruta's work was published a lot of attention was paid to preparation and characterization of such nanogold based catalysts (Röhe et al., 2013; Sreedhala et al., 2015; Lopez et al., 2004; Janssens et al., 2006; Sun et al., 2016).

In general, the catalytic activity of Au increases with decreasing particle size (Dobrosz et al., 2005). According to published works (Haruta, 1997; Zanella et al., 2002) the optimum size of the anchored gold nanoparticles (AuNP) is considered about 5 nm for low-temperature CO oxidation. The activity of supported nanoparticles (NPs) is rather complex and dependent not only on particles size and morphology but also on a combination of other factors such as the interaction between NPs and carrier, dispersion of NPs on the surface and effect of active areas of prepared nanocatalysts (Janssens et al., 2007; Chi et al., 2005; Eindhoven, 2010). Regarding the high reactivity of NPs and their further easier handling, it is preferable to anchor NPs on a support to obtain final nanocomposite catalyst, e.g. $Au/MnO/Al_2O_3$, Au/CeO_2, Au/TiO_2 (Grisel et al., 2002; Chenakin and Kruse, 2018; Wu et al., 2018). The support materials might be classified as inactive (SiO_2, Al_2O_3) or active (TiO_2, Fe_2O_3), which can influence the final catalyst reactivity as well (Schubert et al., 2001).

Although silica is considered as a poor support for NPs embedding, there are also numerous practical benefits of using it as a carrier material because of good thermal stability, chemical inertness and excellent mechanical properties (Veith et al., 2009). Moreover, it was found that addition of even small amounts of active oxides (FeO_x, TiO_2, CeO_2) to the amorphous and mesoporous SiO_2 with anchored nanogold leads to the increase in catalytic activity of the nanocomposite (Beck et al., 2009; Comotti et al., 2006; Chen and Goodman, 2006; Vigneron and Caps, 2016).

AuNP can be prepared by conventional methods such as precipitation and chemical vapour deposition or ''green way'' known as biosynthesis. The biosynthesis is relatively easy, cost-effective and eco-friendly method, because no expensive equipment is required, and toxic chemicals are neither needed nor produced. Different kinds of microorganisms (fungi, yeasts, algae) are able to avoid the toxic influence of metallic ions by reducing them to zerovalent nanoform (Schröfel et al., 2011, 2014; Holišová et al., 2019). This fact was essentially the origin of intentional biosynthesis of inorganic NPs after the onset of nanotechnology on the scientific field. In addition, biosynthetically prepared NPs are formed, stabilized or eventually anchored on bio-support (biological material used in biosynthesis) in one step regarding the fact that biomass can act as a reducing, stabilizing and immobilizing agent.

This work follows on the research of AuNP biosynthesis using brown algae *Diadesmis gallica* (DG) described in (Schröfel et al., 2011; Konvičková et al., 2016). Our previous study confirmed application potential of anchored silver nanoparticles on silica surface in disinfection (Konvičková et al., 2016). Other application for bionanocomposite with extraordinary chemical properties could be found in heterogenous catalysis. The aims of this study are: (i) temperature dependent optimized preparation of nanogold-biosilica composite (Au/DG) with diatoms, (ii) the magnetic modification of as-prepared bionanocomposite by iron oxide (ferrofluid) for increase of catalytic activity of bionanocatalysts and (iii) the first testing of magnetically modified and unmodified AuNP anchored on DG frustules in CO oxidation. Obviously, such designing of bionanocatalysts poses a state-of-the-art interdisciplinary approach with great engagement of bionanotechnology and environmental technology.

2. Experimental

2.1. The temperature-dependent biosynthesis of gold nanoparticles

Cultivation of *Diadesmis gallica* was performed according to (Schröfel et al., 2011; Guillard and Lorenzen, 1972). The gold precursor (1 mM $HAuCl_4$, Carl Roth GmbH + Co. KG, ≥ 99,5%) was mixed with concentrated DG suspension in the ratio 1:1 (Konvičková et al., 2016). Samples were then incubated at 25 °C (DG/Au(25)) and 5 °C (DG/Au(5)) until the colour of the mixture turned ruby red due to the presence of AuNP. After the biosynthesis of AuNP, both samples were separated from the culture media via sedimentation and dried at 37 °C for 24 h.

2.2. Magnetic modification of DG/Au(5) sample

DG/Au(5) sample was magnetically modified by perchloric acid stabilized ferrofluid containing NPs of magnetic iron oxides, using two different methods, i.e., with and without the use of methanol. The first procedure using methanol is the traditional approach employing a transfer of the sample to methanol followed by the addition of ferrofluid (Safarik et al., 2007).

The second later discovered method (without methanol) is based on the simple mixing of the sample with ferrofluid (Safarik et al., 2012). In more detail, in the first procedure, 10 mL of methanol (p.a.) and 1 mL of ferrofluid (concentration 46.2 mg mL^{-1}, pH 1.5) was added to 0.5 g of DG/Au (5). Next, the sample was stirred for two hours in the dark. Magnetically modified sample DG/Au(5)MF (M = methanol, F = ferrofluid) was separated from methanol and suspension residues by a magnetic separator. The sample was washed twice in methanol and dried. In the second procedure, 0.6 g of DG/Au(5) and 2 mL of ferrofluid at the concentration of 46.2 mg mL^{-1} and pH 1.5 were mixed thoroughly and subsequently dried to form DG/Au(5)F composite. Both magnetic composites were stabilized at 60 °C for 24 h.

Magnetic parameters of magnetically modified samples DG/Au(5)MF and DG/Au(5)F were measured by vibrating sample magnetometer (VSM) EV9 at room temperature. Displacement hysteresis loops represent the dependence of the magnetization (M) on the applied magnetic field (H).

2.3. Calcination of magnetically unmodified and modified bionanocomposites

The oxidation of CO was selected as a model reaction for the catalytic activity testing of prepared samples. Given the used methodology and the catalytic process itself, tested samples required several pre-treatments before their using in the catalysis, namely calcination, desired size fraction preparing and activation in the stream of helium. Since the catalytic reaction itself was carried out up to 330 °C, the temperature of calcination was set to 450 °C in air for 4 h. Sufficient difference between the maximum reaction temperature and the temperature of calcination was set with respect to the stability of samples during the whole catalysis procedure.

2.4. Morphological characterization of nanogold-biosilica composites and size distribution of nanoparticles

The diatom cells before and after the biosynthesis of AuNP were observed using an optical microscope (Olympus, CX 31). Size and shape of AuNP in samples were studied by transmission electron microscopes (FEI TecnaiSphera 2) and (Jeol 1200 EX) operating at 120 keV. Small amounts of powder samples were suspended in ethanol and fixed on the grids. The AuNP size distribution was calculated using JMicrovision: Image Analysis Toolbox (www.jmicrovision.com), when at least 250 NP were evaluated per sample.

2.5. Spectroscopic characterization of nanogold-biosilica composites

Contents of gold, silica and iron in composites were determined using atomic emission spectrometry with inductively coupled plasma (ICP-AES, ICP CirosVision, Spectro). The crystalline structure of samples was characterized using X-ray diffraction analysis using Brucker D8 Advance diffractometer (Brucker AXS) working with the Bragg-Brentano geometry and position-sensitive Vantec detector and Krystalloflex K780generator. Cobalt lamp CoKα (λ = 1.7889 Å) was used as a source of radiation. Crystalline phase was identified by PDF-2Release 2004 databases (International Centre for Diffraction Data).

2.6. CO catalytic oxidation

The bionanocomposites after calcination were pressed to tablets under the compressive force of 40 kN, followed by crushing and sieving to get a required fraction in the range from 0.16 to 0.315 mm. Prior to oxidation measurement, the sample was activated in the stream of He during 1 h at 300 °C. The activation is performed in order to expose the active sites and remove the impurities adsorbed from the air.

CO catalytic oxidation was carried out in a tubular reactor (i.d. of 5 mm) with an integral catalyst bed in the 60–330 °C temperature range under the atmospheric pressure. The feed flow rate was 100 mL min^{-1} and contained 2500 ppm CO and 2 mol.% O_2 in He. The catalyst sample of 0.1 g was layered between the inert glass fractions to ensure uniform flow of the gas mixture so that the plug flow was ensured. The input and output concentrations of CO were analysed using gas chromatograph AGILENT 7890A with thermal conductivity detector.

CO conversion was chosen as a measure for the catalytic activity and was calculated using the Eq. (1), where constant total volume flow due to low CO concentration is assumed; c_{COin} is the inlet CO concentration and c_{COout} is the outlet CO concentration.

$$\chi_{CO}(\%) = \frac{c_{COin} - c_{COout}}{c_{COin}} \quad (1)$$

3. Results and discussion

3.1. Characterization of nanogold-biosilica composites after the temperature-dependent biosynthesis

The probable mechanism of AuNP fabrication using brown algae has been described in previous publications (Schröfel et al., 2011; Konvičková et al., 2016). Gold ions present in the suspension are reduced using biomolecules (for example extracellularly polysaccharides) contained in the silica algae. Biosynthesized AuNPs are subsequently associated and stabilized on the surface of diatomaceous frustules. During biosynthesis, the influence of two different temperatures (25 °C and 5 °C) on the size and homogeneity of nanogold particles in the composite was tested. The samples of DG with AuNP for both temperatures changed its colour from brown through purple to dee purple (Fig. A.1 Supplementary Data) due to the presence of bionanogold particles.

Whole bioreduction process of gold ions in DG/Au(25) sample at 25 °C took app. 48 h. Biosynthesis of AuNP at 5 °C took 96 h. That was the expected result because, as it is generally known, the temperature influences activity and mobility of ions and thus subsequent formation of NPs (Kumari et al., 2016).

TEM (transmission electron microscopy) micrographs revealed that spherical AuNP biosynthesised at 5 °C have narrow size and more homogeneous size distribution than AuNP biosynthesised at 25 °C. The average particle size is around 15 nm for DG/Au(5) sample and 17 nm for DG/Au(25) (Figs. A.2 and A.3 Supplementary Data). The smaller size of

AuNP prepared at 5 °C may be caused by the increase in the activation energy of Au cluster nucleation which leads to a slower growth of Au nuclei in the solution (Polte, 2015). Because AuNP in DG/Au(5) sample were smaller (mostly 14 nm) and their size distribution was homogenous, higher efficacy of prepared bionanocomposite for catalysis in lower temperature can be expected (Dobrosz et al., 2005).

ICP-AES analysis revealed the total content of gold in DG/Au(25) and DG/Au(5) samples as 7.61 ± 0.76 wt.% and 6.46 ± 0.65 wt.%, respectively. Regarding standard deviation, it can be considered that the content of gold is almost identical in both samples. Catalytic activity will be influenced mainly by NPs size and dispersity on frustules surface.

3.2. Calcination and its effect on the nanogold-biosilica composites

Prepared bionanocomposite is a complex system full of organic parts, which are unstable at high temperatures and can decrease the catalytic activity of samples (Yang et al., 2015). For this reason, the calcination is a necessary step. The calcination of the sample guarantees its stability during the CO oxidation process itself, which also works at elevated temperatures (up to 300 °C), therefore the calcination temperature should be at least 450 °C. During the calcination process, the size of NPs could increase (Kratošová et al., 2016). Therefore, it is useful to prepare initial NPs with the smallest possible size distribution before calcination and catalysis.

3.2.1. DG/Au(25) and DG/Au(5) after calcination

TEM analysis confirmed the growth of NPs on the biosilica surface of DG in DG/Au(25) and DG/Au(5) after calcination. For both samples, NPs size distribution was fitted by the log-normal curve, which pointed on the polydispersity of AuNP anchored on frustules (Fig. 1). The size of NPs in DG/Au (25) increased to an average size of 21 nm after calcination, with most occurred NPs of 19–21 nm (see Fig. 1b). High temperature during the calcination process caused an increase of AuNP size by approximately 4 nm.

The average size of AuNP in DG/Au(5) was still 15 nm after the calcination, but now in the polydisperse system of nanogold on silica frustules. The nanogold size was around 16–18 nm, which is evident from the histogram in Fig. 1d.

With regard to the $HAuCl_4$ precursor in biosynthesis experiments, we may suppose some poisoning effect of the residual chlorides. Residual chloride anions may cause the agglomeration of AuNP by forming Au-Cl-Au bridges and change the particle size distribution during the calcination process (Dobrosz et al., 2005). Anyhow, it seems to be useful to wash the samples to remove chloride ions after the biosynthesis of AuNP.

During the calcination, organic parts are burned at high temperature leading to the loss of weight which was in our

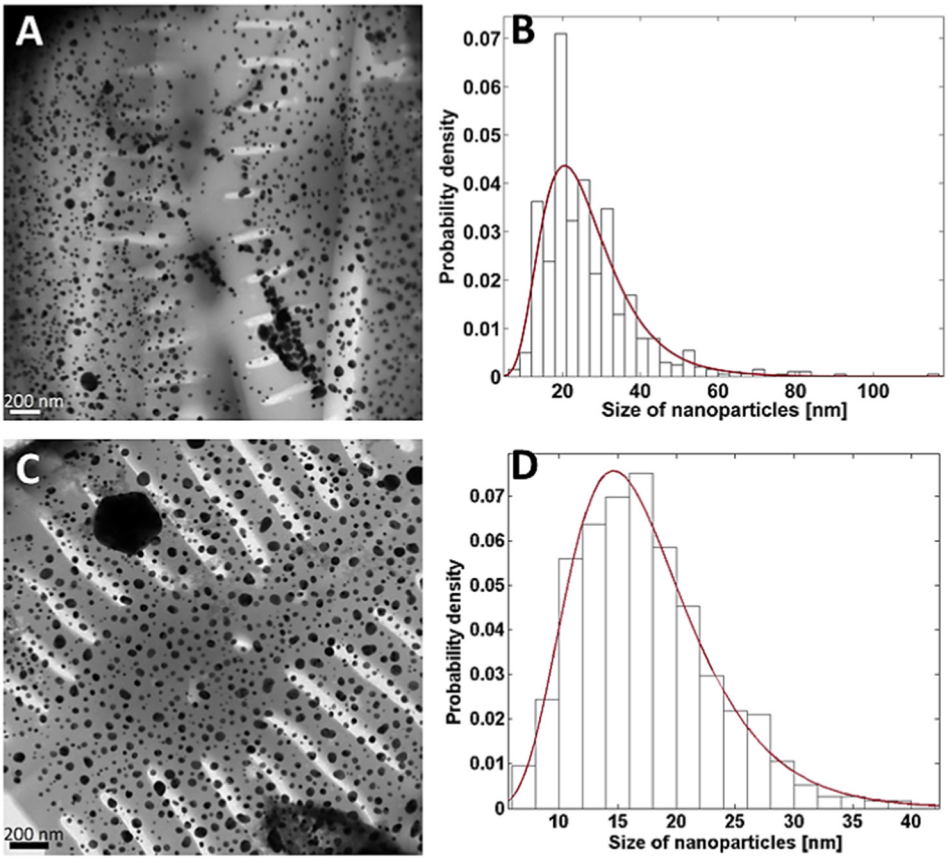

Fig. 1 TEM micrograph of AuNP associated on diatom frustules of DG/Au(25) (a) and DG/Au(5) (c) after the calcination and size distribution histogram of DG/Au(25) (b) and DG/Au(5) (d).

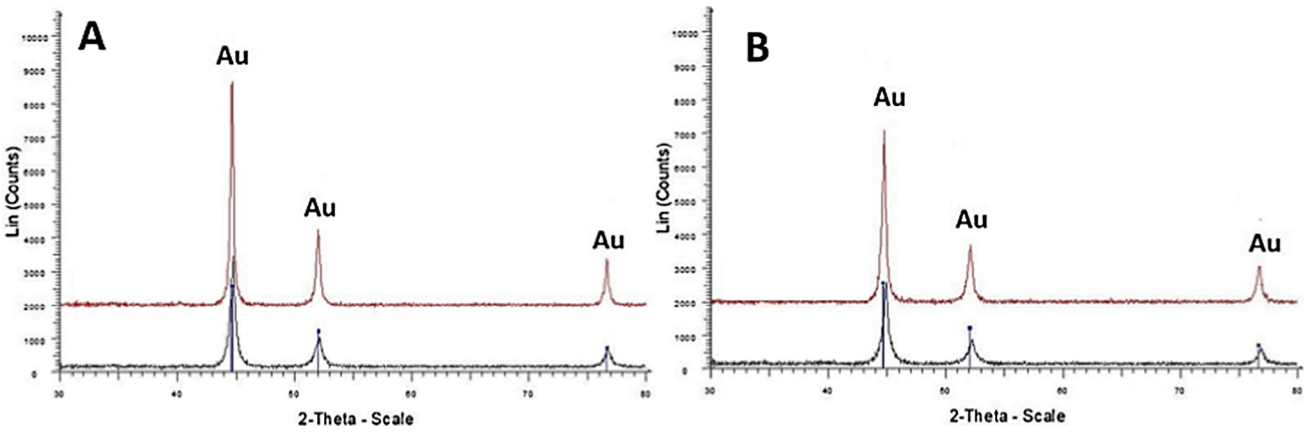

Fig. 2 XRD patterns of DG/Au(25) (a) and DG/Au(5) (b) before – black line and after calcination – red line.

samples 48% and 57% for DG/Au(25) and DG/Au(5), respectively. Due to the calcination, the content of gold in samples was higher than in non-calcined, i.e.16.6 ± 1.7 wt.% and 15.5 ± 1.5 wt.% in DG/Au(25) and DG/Au(5), respectively.

The crystallographic analysis confirmed that only the gold remained after the calcination in the samples, the silica was not detected due to the amorphous nature (Wang et al., 2013). The crystalline structure of AuNP in samples DG/Au (25) and DG/Au(5) before and after calcination was studied using X-ray diffraction (XRD). The XRD pattern (Fig. 2) showed 3 characteristic diffraction peaks at 2 theta values 45°, 52° and 77° corresponding to (1 1 1), (2 0 0) and (2 2 0) planes of cubic crystal structure of gold (PDF number 04-0784) for DG/Au samples. Intensities of Au peaks are higher after calcination which is related to growing particles size and crystalline character.

3.2.2. Magnetically modified sample of DG/Au(5) after calcination

To improve properties regarding stability and catalytic efficiency, the treatment of composite with ferrofluid was assessed as an optimisation step. It was previously reported (Vigneron and Caps, 2016) that promoter reducible oxides (FeO_x, TiO_2, NiO) can improve the efficacy and thereby they turn on the catalytic cycle because they are also the source of oxygen needed for the CO oxidation.

For this experiment, DG/Au(5) sample was only used because of better physical properties (smaller size of NPs, narrower distribution, higher homogeneity) as described above. Finally, two types of samples were prepared: DG/Au(5)MF and DG/Au(5)F by a different method of magnetic modification (with and without the use of methanol).

The TEM revealed a heterogeneous size distribution of spherical AuNP for both magnetically modified samples after calcination. The average size of nanogold in DG/Au(5)MF was 23 nm. The most frequently represented size of AuNP was 23 nm (Fig. 3b). The average size of spherical nanogold in DG/Au(5)F was 20 nm. The most frequently poses size of AuNP was approximately 16–20 nm (Fig. 3d).

Burning of organic parts during calcination process leads to the loss of weight in samples which was 52% and 43% for DG/Au(5)F and DG/Au(5)MF, respectively. The total amount of Au and Fe in magnetically modified bionanocomposite after calcination was measured by ICP-AES. Preparation of nanogold-biosilica composites proceeded at laboratory conditions and therefore we talk about low-volume preparation of sample (app. 1 g). Two samples with AuNP were prepared using the same method of biosynthesis (at 5 °C) for each magnetic modification (with and without methanol). DG/Au(5)F contained 3.70 ± 0.37 wt.% Au and 13.80 ± 1.00 wt.% Fe after the calcination. In the case of DG/Au(5)MF sample, 6.52 ± 0.66 wt.% Au and 10.40 ± 0.80 wt.% Fe was measured. Differences in content of Au in the magnetically modified samples may be caused by the irregular distribution of Au due to the static method of preparation. This deficiency can be avoided by continuously mixing the solution at the time during the bioreduction of Au ions. The lower content of Fe in the case of DG/Au(5)MF was predicted because 1 mL of ferrofluid was added to 0.5 g of pure nanogold-biosilica composite, while in another modification protocol 0.6 g of composite was mixed with 2 mL of ferrofluid obtaining DG/Au(5)F sample. Theoretically, the amount of iron is 1.7× higher than in the sample modified with methanol. This result has not been achieved due to the different method of preparation. Method of magnetic modification of sample with methanol has a longer tradition and was earlier verified on various samples as well as on diatoms (DG) (Safarik et al., 2007; Kratošová et al., 2013). Surprisingly, the direct mixing of ferrofluid with bionanocomposite was less effective than in the case of methanol method.

Ferrofluid used for composites modification contains magnetic iron oxide nanoparticles (Safarik et al., 2012). Using XRD analysis for DGAu(5)MF and DGAu(5)F magnetite and maghemite diffraction lines were not observed before their calcination (Fig. 4), but only in the case of DGAu(5)F sample the presence of ferrosilite ($FeSiO_3$) was revealed. XRD study proved these expectations and showed presence of magnetite in magnetically modified samples after their calcination (Fig. 4). Higher intensities of iron oxides peaks can be caused by growing particles size and crystalline character.

However, due to similar positions of maghemite and magnetite diffraction lines in the XRD pattern, it is difficult to differentiate between them.

The response of magnetic NPs in ferrofluid to external magnetic fields reflects characteristic different spin dynamical processes compared to those of their bulk counterparts. In order

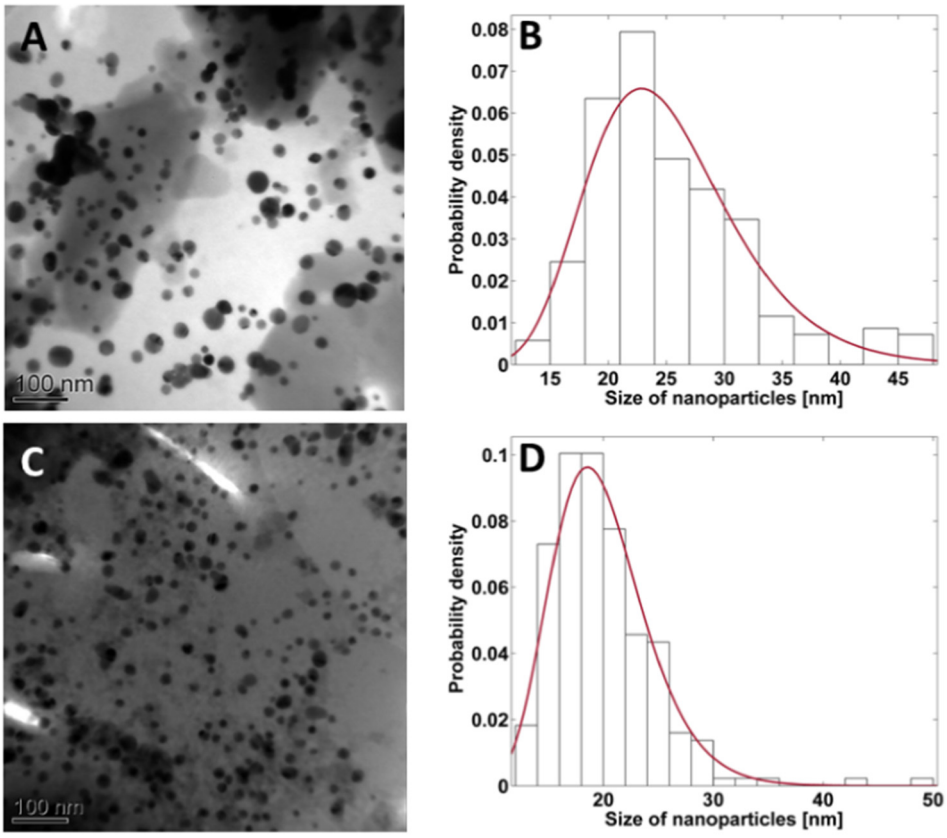

Fig. 3 TEM micrograph of AuNP associated on diatom frustules of DG/Au(5)MF (a) with size distribution histogram (b) and DG/Au (5)F (c) with size distribution histogram (d) after calcination.

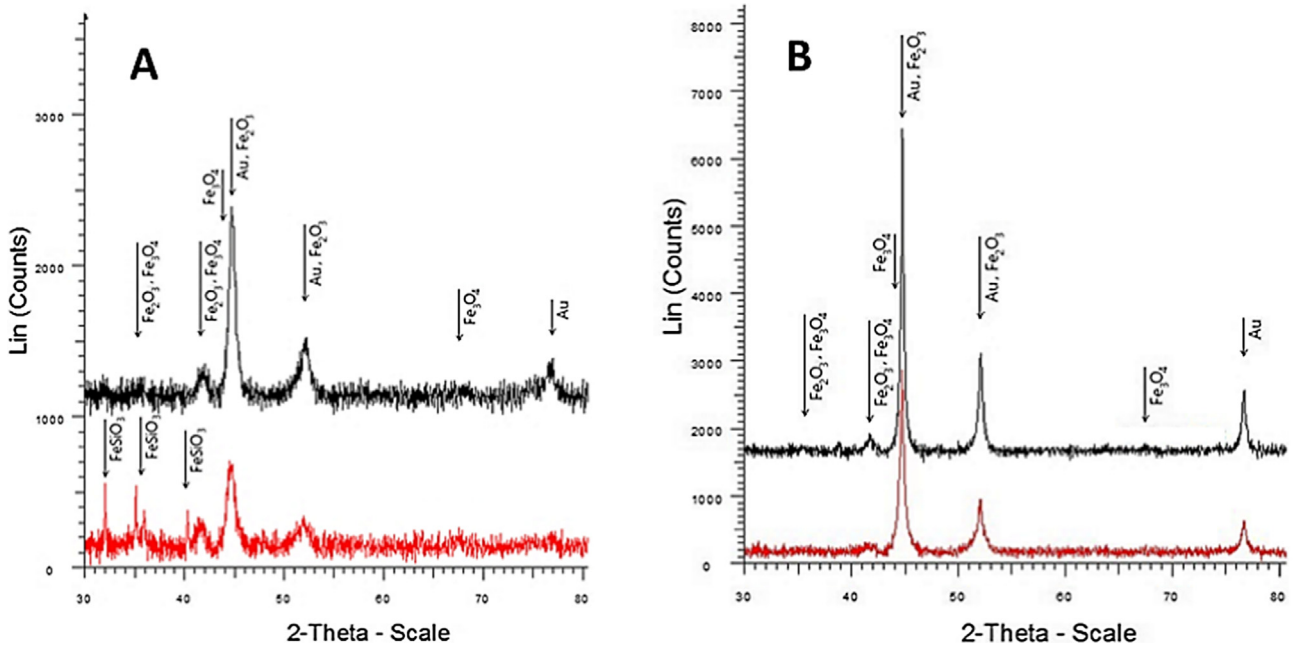

Fig. 4 X-ray diffraction of DGAu(5)F (a) and DGAu(5)MF (b)- red line and after calcination - black line.

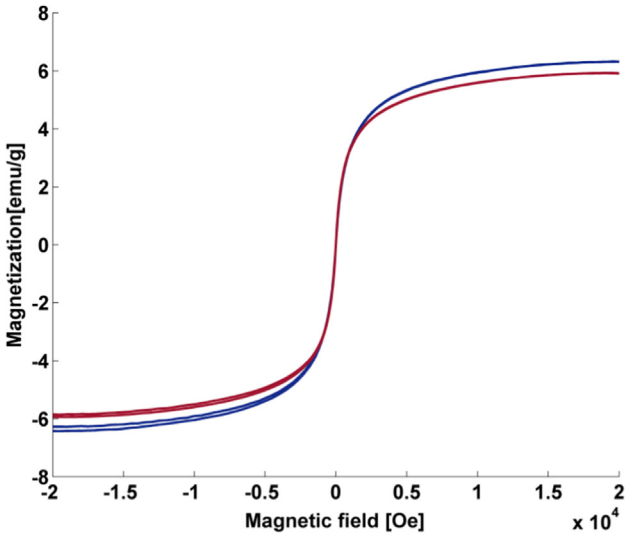

Fig. 5 Magnetic curves of magnetically modified samples in the external magnetic field for DGAu(5)MF (blue line) and for DGAu (5)F (red line) after calcination.

to test if the obtained magnetically modified DG/Au(5)MF and DG/Au(5)F could be used in the magnetic separation procedures, samples were tested using VSM. The test with magnetization measurements as a function of the applied magnetic field was performed. At room temperature, the field-dependent magnetization curves of all prepared magnetic composites show their ferromagnetic properties (Fig. 5) and thus their ability to be influenced and manipulated in the external magnetic field, which could be beneficial in future application of catalysts.

Regarding magnetization curves, samples have been already saturated in the applied external magnetic field (15.000 Oe). Both the curves have similar shapes, assuming similar magnetic behaviour of samples. The values of magnetization saturation (Ms) and coercive field (Hc) are shown in the Table 1.

3.3. CO catalytic oxidation over prepared bionanocomposites

The catalytic activity of non-magnetic (DG/Au(25), DG/Au (5)) and magnetically modified (DG/Au(5)F, DG/Au(5)MF) nanogold-biosilica samples was tested for catalytic oxidation of CO at temperatures 60–330 °C (Fig. 6).

The conversion of CO at 300 °C was 58% in the presence of DG/Au(25) and 60% when using DG/Au(5). The sample DG/Au(5) with smaller and uniform AuNP were presented (Table 2), did not show a significant difference in catalytic activity compared to the sample DG/Au(25) with bigger NPs.

Table 1 Basic magnetic parameters of DG/Au(5)MF and DG/Au(5)F composites.

Sample	M_s [emu/g]	H_c [Oe]
DG/Au(5)MF	4.95	1.45
DG/Au(5)F	4.09	3.86

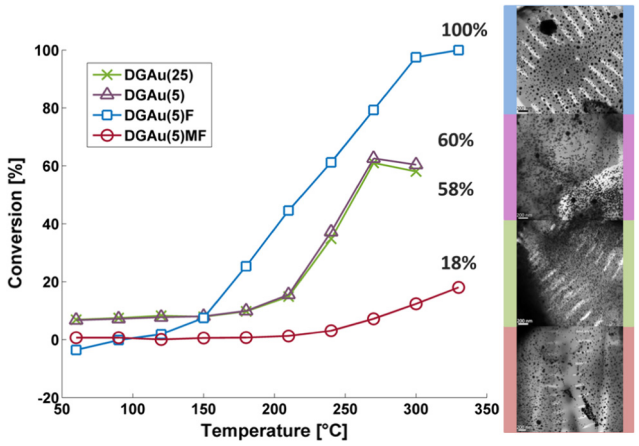

Fig. 6 Temperature dependences of CO conversion in the presence of bionanocomposites as the catalyst.

The lower catalytic efficiency of both samples in CO oxidation could be caused by residual Cl^- on the nanogold catalyst lead to deactivation of active sites in nanogold-biosilica composite. This phenomenon was confirmed in the work by (Chen et al., 2017). Moreover, the TEM analysis of samples after catalytic tests confirmed the unification of size and distribution of NPs for both samples as it is seen in Fig. 7. In the DG/Au(5) sample, the average size of AuNP was 20 nm and in the sample of DG/Au(25) was 23 nm after the catalytic test. The most prevalent size of NPs was 22 nm for both samples.

Results show that the size of AuNP increased for both samples (DG/Au(25) and DG/Au(5)) after catalytic tests. The reaction between $HAuCl_4$ and some acidic oxides, e.g. with negatively charged silica surfaces (isoelectric point 1, 2) is usually inactive (Dobrosz et al., 2005) and leads to relatively weak interaction between AuNP and inactive supports. This can cause the agglomeration of NPs, which may lead to decreasing catalytic activity in CO oxidation. To avoid agglomeration, several precipitation agents such as ammonia or urea have been investigated in the deposition-precipitation method. The use of ammonia causes the formation of gold ammine cationic complex, which reacts with the negatively charged silica surface (Dobrosz et al., 2005). Another approach is the limitation of particles size by capturing in the pore with controlled uniform pore system as present in zeolites or mesoporous silica (Chen et al., 2017). Stabilization of NPs via cellular debris seems to be sufficient at normal temperatures but to avoid unwanted growth at high temperatures it is probably better to anchor the particles more efficiently. On the other hand, it was reported that trioctahedral AuNP the size of 45 nm and 100 nm could be catalytically active as well, although the optimum of AuNP for CO oxidation is considered up to 5 nm (Sreedhala et al., 2015).

It was expected that magnetic modification would increase the catalytic activity of the bionanocomposites. Generally, the molecules of CO are adsorbed on the AuNP surface in Au/oxide-matrix based nanocomposite and the dissociation of O_2 occurs at the metal/support interface (between AuNP and SiO_2). Molecules of O_2 are stable at room temperature and, therefore, higher temperature is needed for their dissociation. In the case of AuNP on inactive support, the active sites on the AuNP surface are inhibited by the CO molecules due to the missing dissociated oxygen. By adding the reducible oxide

Table 2 Physico-chemical properties of nanogold-biosilica composites.

Catalyst	Au NP size[a] [nm]			Fe/Au ratio
	As prepared	After calcination	After catalytic test	Weight
DG/Au(5)	15	15	20	n.d.
DG/Au(25)	17	21	23	n.d.
DG/Au(5)F	n.d.	20	23	3.7
DG/Au(5)MF	n.d.	23	23	1.6

[a] Average Au nanoparticle size determined from TEM.

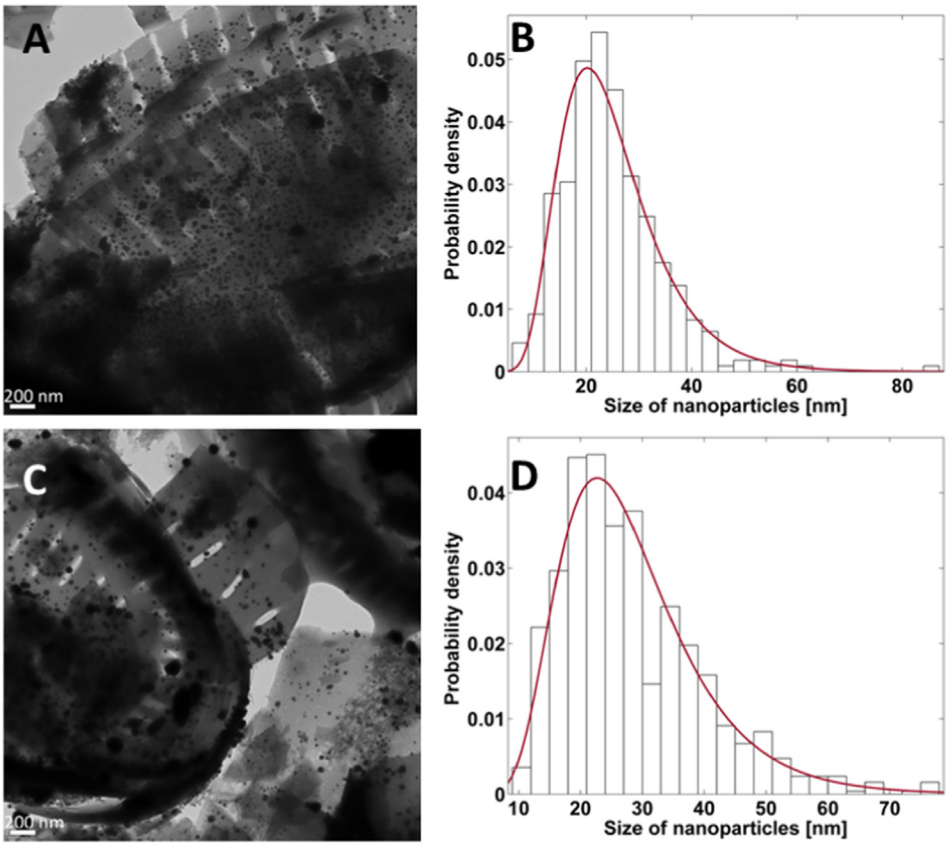

Fig. 7 TEM micrograph of AuNP associated on diatom frustules of DG/Au(25) (a) with size distribution histogram (b) and DG/Au(5) (c) with size distribution histogram (d) after catalysis.

to metal/inactive-supports, the new interface between AuNP and reducible oxides is formed and regarded as the location of the most active sites in CO oxidation. The release of oxygen from the matrix causes the presence of oxygen vacancy at the interface of AuNP/reducible oxide, where others O_2 can be dissociated. This process is called oxygen activation via a redox-type mechanism. Dissociated O_2 molecules then react with the adsorbed CO molecules on the AuNP surface via Langmuir-Hinshelwood mechanism and the catalytic process continues in the cycle. In this way, the reaction runs at lower temperatures, since oxygen is provided from promoter reducible oxide, in our case probably from FeO_x. Moreover, modification with promoter reducible oxides could inhibit the unwanted growth of NPs at high temperature (Beck et al., 2009).

DG/Au(5)F showed excellent catalytic effect in comparison with the nonmagnetic sample when 98% conversion of CO at 300 °C was observed. Moreover, CO molecules were completely converted at 330 °C. However, DG/Au(5)MF prepared using the method with methanol, did not confirm the increase of catalytic activity in CO oxidation. CO conversion at 300 °C was only 15% (18% CO conversion at 330 °C). The conversion was even lower than for unmodified samples. With regard to these results, it was surprising that the TEM analysis revealed the similar size distribution after catalytic experiments (Fig. 8). The average and the most frequently represented size was 23 nm in both magnetically modified samples. AuNP size distribution was fitted with the lognormal curve for both samples, which pointed to the polydisperse system.

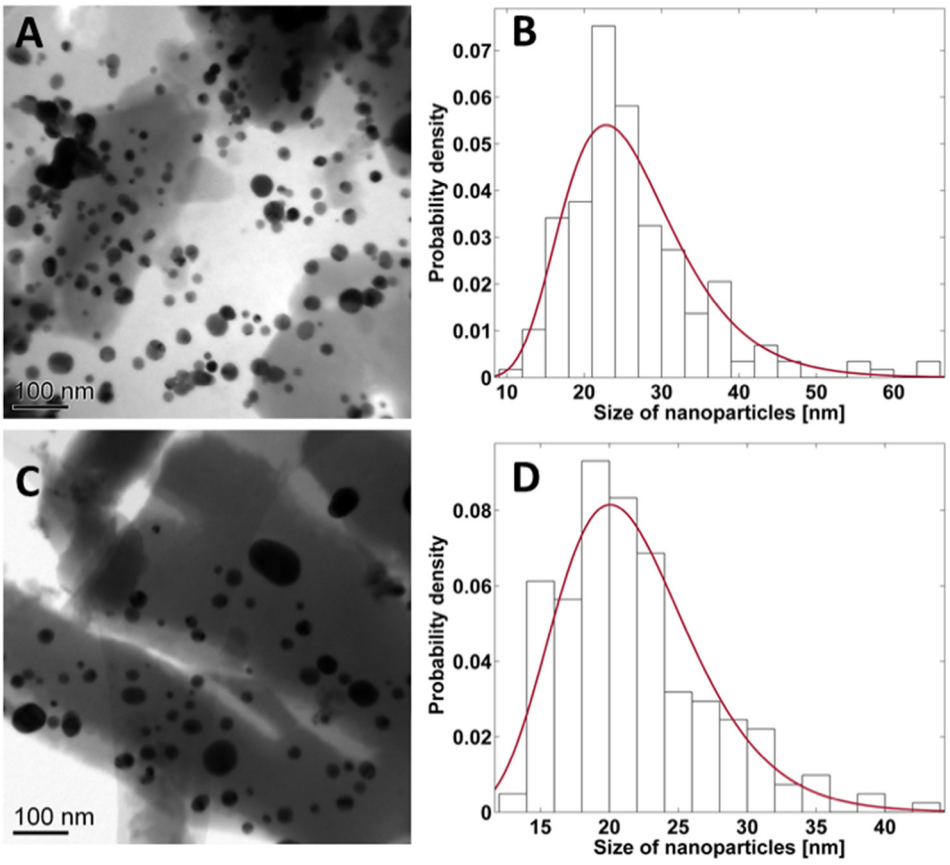

Fig. 8 TEM micrograph of AuNP associated on diatom frustules of DG/Au(5)MF (a) with size distribution histogram (b) and DG/Au (5)F (c) with size distribution histogram (d) after catalysis.

We can assume that the method of magnetic modification influences the catalytic activity of the sample. Methanol used in the preparation of DG/Au(5)MF sample caused a decrease in catalytic activity. CO oxidation was found to be directly related to the number of perimeter sites, i.e., the number of bifunctional gold-support sites (Vigneron and Caps, 2016). The ratio of Fe to Au (Table 2) was higher in the case of DG/Au(5)F, which may indicate a larger amount of active sites at the Au/promoter reducible oxide interface.

There are several studies, which are focused on preparation of metallic NPs and their using for CO oxidation. For example work of (Qian et al., 2007), deposition-precipitation method for preparing of AuNP (7–15 nm) from $HAuCl_4$ precursor supported on SiO_2 were used. 100% CO conversion was achieved at 526 °C. 100% CO conversion at 60 °C were reported by (Ren et al., 2012). As nanocatalyst, they used $Au/CeO_2/SiO_2$ nanocomposite prepared by the deposition-precipitation method. AuNP size was 2–5 nm. In the work of Xu et al., the catalytic activity of Au/SiO_2 and $Au/FeO_x/SiO_2$ nanocomposites prepared by deposition-precipitation method was studied as well. Sizes of AuNP were 3–13 nm for Au/SiO_2 sample and 1–3 nm for $Au/FeO_x/SiO_2$ sample. Total conversion of CO over Au/SiO_2 and $Au/FeO_x/SiO_2$ nanomaterials was observed at 475 °C and 227–262 °C, respectively (Xu et al., 2010). Reducible oxides enhanced electron interactions, lead to the enlargement of the reactive species and finally to the increase of nanocomposite catalytic activity in CO oxidation (Comotti et al., 2006; Chen and Goodman, 2006; Vigneron and Caps, 2016). Only in one study, biosynthesized metallic nanoparticles were tested for CO oxidation. Ag nanoparticles prepared using plant extract were anchored on chemically prepared CeO_2 support. Moreover, the size of Ag nanoparticles (18 nm) was optimized by microwave irradiation. Completely conversion of CO over Ag/CeO_2 nanomaterial was achieved at 200 °C (Yang et al., 2015).

Bionanocomposites prepared by bioreduction and magnetically modified had comparable and satisfactory catalytic activity with regard to the above-mentioned articles despite to higher particle size. With respect to the physical and chemical methods of NPs preparation described in other works, the preparation of the bionanocatalyst in this study seems to be simple, environmentally friendly and economical undemanding. The main advantageous of AuNP biosynthesis using DG is forming and direct embedding of the nanogold on the 3D structure of the biosilica frustules in one step. It is not necessary chemically prepared matrix for NPs anchoring or stabilizer agents. The final nanomaterial is functional bionanocomposite (magnetically responsive), which shows catalytic activity in CO oxidation and can be further utilized as nanocatalyst for other degradation reactions (organic or inorganic compounds).

4. Conclusions

Bionanocomposite Au/DG was prepared using an eco-friendly approach called biosynthesis. The advantage of this approach

is the simultaneous formation and direct embedding of gold nanoparticles on the 3D porous biosilica structure at mild conditions. Silica frustules of brown algae were employed as a support for AuNP, which are considered as good mechanical and inert matrix. Nanogold-biosilica composite was further tested as a catalyst in the CO oxidation. Moreover, a simple magnetic modification of nanogold-biosilica composite by ferrofluid was used successfully. The addition of active iron oxide in the form of ferrofluid caused the increase of efficacy of modified composite in CO oxidation. 100% conversion of CO was achieved at 330 °C in the presence of the magnetically modified bionanocomposite containing AuNP (app. 20 nm). The article presents an underlying interdisciplinary study including bionanotechnology, nanotechnology and diatom nanotechnology with significant impact on environmental-based research.

Acknowledgements

The English language in the article "Magnetically modified nanogold-biosilica composite as an effective catalyst for CO oxidation" was reviewed by Dr. Oldrich Motyka. We would like to thank Dr. Kateřina Mamulová Kutláková for carrying X-ray diffraction analysis and Ing. Šárka Tomisová for carrying atomic emission spectroscopy.

Funding

This work was realized thanks to support of SGS Project SP2016/72, SGS Project SP2018/72 and by the project LTC17020 and CZ.02.1.01/0.0/0.0/16_019/0000853 of the Ministry of Education, Youth and Sports of the Czech Republic.

Appendix A. Supplementary material

Supplementary data to this article can be found online at https://doi.org/10.1016/j.arabjc.2018.12.002.

References

Beck, A., Guczi, L., Frey, K., 2009. Role of promoting oxide morphology dictating the activity of Au/SiO_2 catalyst in CO oxidation. Gold Bull. 42, 5–12.

Chen, M.S., Goodman, D.W., 2006. Structure-activity relationships in supported Au catalysts. Catal. Today 111, 22–33. https://doi.org/10.1016/j.cattod.2005.10.007.

Chen, Y.H., Mou, C.Y., Wan, B.Z., 2017. Ultrasmall gold nanoparticles confined in zeolite Y: preparation and activity in CO oxidation. Appl. Catal. B Environ. 218, 506–514. https://doi.org/10.1016/j.apcatb.2017.06.083.

Chenakin, S., Kruse, N., 2018. Combining XPS and ToF-SIMS for assessing the CO oxidation activity of Au/TiO_2 catalysts. J. Catal. 358, 224–236. https://doi.org/10.1016/j.jcat.2017.12.010.

Chi, Y.S., Lin, H.P., Mou, C.Y., 2005. CO oxidation over gold nanocatalyst confined in mesoporous silica. Appl. Catal. A Gen. 284, 199–206. https://doi.org/10.1016/j.apcata.2005.01.034.

Comotti, M., Li, W.-C., Spliethoff, B., Schüth, F., 2006. Support effect in high activity gold catalysts for CO oxidation. J. Am. Chem. Soc. 128, 917–924. https://doi.org/10.1021/ja0561441.

Dobrosz, I., Jiratova, K., Pitchon, V., Rynkowski, J.M., 2005. Effect of the preparation of supported gold particles on the catalytic activity in CO oxidation reaction. J. Mol. Catal. A Chem. 234, 187–197. https://doi.org/10.1016/j.molcata.2005.02.032.

Eindhoven, T.U., 2010. A computational study of catalysis by gold in applications of CO oxidation. https://doi.org/10.6100/IR685817.

Grisel, R., Weststrate, K.J., Gluhoi, A., Nieuwenhuys, B.E., 2002. Catalysis by gold nanoparticles. Gold Bull. 35, 39–45. https://doi.org/10.1007/BF03214836.

Guillard, R.R.L., Lorenzen, C.J., 1972. Yellow-green algae with chlorophyllide C1,2. J. Phycol. 8, 10–14. https://doi.org/10.1111/j.1529-8817.1972.tb03995.x.

Haruta, M., 1997. Size- and support-dependency in the catalysis of gold. Catal. Today 36, 153–166. https://doi.org/10.1016/S0920-5861(96)00208-8.

Haruta, M., Kobayashi, T., Sano, H., Yamada, N., 1987. Novel gold catalysts for the oxidation of carbon monoxide at a temperature far below 0 °C. Chem. Lett. 16, 405–408. https://doi.org/10.1246/cl.1987.405.

Holišová, V., Urban, M., Kolenčík, M., Němcová, Y., Schröfel, A., Peikertová, P., Slabotinský, J., Kratošová, G., 2019. Biosilica-nanogold composite: easy-to-prepare catalyst for soman degradation. Arab. J. Chem. 12, 262–271.

Janssens, T.V.W., Carlsson, A., Puig-Molina, A., Clausen, B.S., 2006. Relation between nanoscale Au particle structure and activity for CO oxidation on supported gold catalysts. J. Catal. 240, 108–113. https://doi.org/10.1016/j.jcat.2006.03.008.

Janssens, T.V.W., Clausen, B.S., Hvolbæk, B., Falsig, H., Christensen, C.H., Bligaard, T., Nørskov, J.K., 2007. Insights into the reactivity of supported Au nanoparticles: combining theory and experiments. Top. Catal. 44, 15–26. https://doi.org/10.1007/s11244-007-0335-3.

Konvičková, Z., Schröfel, A., Kolenčík, M., Dědková, K., Peikertová, P., Žídek, M., Seidlerová, J., Kratošová, G., 2016. Antimicrobial bionanocomposite–from precursors to the functional material in one simple step. J. Nanoparticle Res. 18, 368. https://doi.org/10.1007/s11051-016-3664-y.

Kratošová, I.V.G., Natšinová, M., Holišová, V., Obalová, L., Chromčáková, Ž., 2016. Transmission electron microscopy observation of bionanogold used for preliminary N_2O decomposition testing. Adv. Sci. Lett. 22, 631–636. https://doi.org/10.1166/asl.2016.6992.

Kratošová, G., Vávra, I., Kadilak, A., Schröfel, A., 2013. Synthesis of metallic nanoparticles by diatoms – prospects and applications. Green Biosynth. Nanoparticles Mech. Appl., 63–80 https://doi.org/10.1079/9781780642239.0061.

Kumari, M., Mishra, A., Pandey, S., Singh, S.P., Chaudhry, V., Mudiam, M.K.R., Shukla, S., Kakkar, P., Nautiyal, C.S., 2016. Physico-chemical condition optimization during biosynthesis lead to development of improved and catalytically efficient gold nano particles. Sci. Rep. 6. https://doi.org/10.1038/srep27575.

Lopez, N., Janssens, T.V.W., Clausen, B.S., Xu, Y., Mavrikakis, M., Bligaard, T., Nørskov, J.K., 2004. On the origin of the catalytic activity of gold nanoparticles for low-temperature CO oxidation. J. Catal. 223, 232–235. https://doi.org/10.1016/j.jcat.2004.01.001.

Polte, J., 2015. Fundamental growth principles of colloidal metal nanoparticles – a new perspective. CrystEngComm. 17, 6809–6830. https://doi.org/10.1039/C5CE01014D.

Prockop, L.D., Chichkova, R.I., 2007. Carbon monoxide intoxication: an updated review. J. Neurol. Sci. 262, 122–130. https://doi.org/10.1016/j.jns.2007.06.037.

Qian, K., Huang, W., Jiang, Z., Sun, H., 2007. Anchoring highly active gold nanoparticles on SiO_2 by CoOx additive. J. Catal. 248, 137–141. https://doi.org/10.1016/j.jcat.2007.02.010.

Ren, L.H., Zhang, H.L., Lu, A.H., Hao, Y., Li, W.C., 2012. Porous silica as supports for controlled fabrication of $Au/CeO_2/SiO_2$ catalysts for CO oxidation: Influence of the silica nanostructures. Microp. Mesop. Mater. 158, 7–12. https://doi.org/10.1016/j.micromeso.2012.03.010.

Röhe, S., Frank, K., Schaefer, A., Wittstock, A., Zielasek, V., Rosenauer, A., Bäumer, M., 2013. CO oxidation on nanoporous gold: a combined TPD and XPS study of active catalysts. Surf. Sci. 609, 106–112. https://doi.org/10.1016/j.susc.2012.11.011.

Safarik, I., Lunackova, P., Mosiniewicz-Szablewska, E., Weyda, F., Safarikova, M., 2007. Adsorption of water-soluble organic dyes on ferrofluid-modified sawdust. Holzforschung 61, 247–253. https://doi.org/10.1515/HF.2007.060.

Safarik, I., Horska, K., Pospiskova, K., Safarikova, M., 2012. One-step preparation of magnetically responsive materials from non-magnetic powders. Powder Technol. 229, 285–289. https://doi.org/10.1016/j.powtec.2012.06.006.

Schröfel, A., Kratošová, G., Bohunická, M., Dobročka, E., Vávra, I., 2011. Biosynthesis of gold nanoparticles using diatoms-silica-gold and EPS-gold bionanocomposite formation. J. Nanoparticle Res. 13, 3207–3216. https://doi.org/10.1007/s11051-011-0221-6.

Schröfel, A., Kratošová, G., Šafařík, I., Šafaříková, M., Raška, I., Shor, L.M., 2014. Applications of biosynthesized metallic nanoparticles - A review. Acta Biomater. 10, 4023–4042. https://doi.org/10.1016/j.actbio.2014.05.022.

Schubert, M.M., Hackenberg, S., van Veen, A.C., Muhler, M., Plzak, V., Behm, R.J., 2001. CO oxidation over supported gold catalysts—"inert" and "active" support materials and their role for the oxygen supply during reaction. J. Catal. 197, 113–122. https://doi.org/10.1006/jcat.2000.3069.

Sreedhala, S., Sudheeshkumar, V., Vinod, C.P., 2015. Oxidation catalysis by large trisoctahedral gold nanoparticles: mind the step! Catal. Today 244, 177–183. https://doi.org/10.1016/j.cattod.2014.02.049.

Sun, X., Su, H., Lin, Q., Han, C., Zheng, Y., Sun, L., Qi, C., 2016. Au/Cu–Fe–La–Al_2O_3: a highly active, selective and stable catalysts for preferential oxidation of carbon monooxide. Appl. Catal. A Gen. 527, 19–29. https://doi.org/10.1016/j.apcata.2016.08.014.

Veith, G.M., Lupini, A.R., Rashkeev, S., Pennycook, S.J., Mullins, D. R., Schwartz, V., Bridges, C.A., Dudney, N.J., 2009. Thermal stability and catalytic activity of gold nanoparticles supported on silica. J. Catal. 262, 92–101. https://doi.org/10.1016/j.jcat.2008.12.005.

Vigneron, F., Caps, V., 2016. Evolution des méthodes chimiques de préparation des catalyseurs d'oxydation à l'or. Comptes Rendus Chim. 19, 192–198. https://doi.org/10.1016/j.crci.2015.11.015.

Wang, Y., Cai, J., Jiang, Y., Jiang, X., Zhang, D., 2013. Preparation of biosilica structures from frustules of diatoms and their applications: Current state and perspectives. Appl. Microbiol. Biotechnol. 97, 453–460. https://doi.org/10.1007/s00253-012-4568-0.

Wu, Z., Mullins, D.R., Allard, L.F., Zhang, Q., Wang, L., 2018. CO oxidation over ceria supported Au 22 nanoclusters: shape effect of the support. Chinese Chem. Lett. https://doi.org/10.1016/j.cclet.2018.01.038.

Xu, H., Chu, W., Luo, J., Liu, M., 2010. New Au/FeOx/SiO_2 catalysts using deposition-precipitation for low-temperature carbon monoxide oxidation. Catal. Commun. 11, 812–815. https://doi.org/10.1016/j.catcom.2010.02.023.

Yang, F., Huang, J., Odoom-Wubah, T., Hong, Y., Du, M., Sun, D., Jia, L., Li, Q., 2015. Efficient Ag/CeO_2 catalysts for CO oxidation prepared with microwave-assisted biosynthesis. Chem. Eng. J. 269, 105–112. https://doi.org/10.1016/j.cej.2015.01.062.

Zanella, R., Giorgio, S., Henry, C.R., Louis, C., 2002. Alternative methods for the preparation of gold nanoparticles supported on TiO_2. J. Phys. Chem. B. 106, 7634–7642. https://doi.org/10.1021/jp0144810.